Design of a radiation tolerant system for total ionizing dose monitoring using floating gate and RadFET dosimeters

Rudy Ferraro, Salvatore Danzeca, Matteo Brucoli, Alessandro Masi, Markus Brugger, Luigi Dilillo

Published by IOP Publishing for Sissa Medialab

Received: *November 14, 2016*
Revised: *January 19, 2017*
Accepted: *March 7, 2017*
Published: *April 4, 2017*

Topical Workshop on Electronics for Particle Physics,
26–30 September 2016,
Karlsruhe Institute of Technology (KIT), Karlsruhe, Germany

Design of a radiation tolerant system for total ionizing dose monitoring using floating gate and RadFET dosimeters

R. Ferraro,[a,c,1] **S. Danzeca,**[a] **M. Brucoli,**[a,b] **A. Masi,**[a] **M. Brugger**[a] **and L. Dilillo**[c,d]

[a] *CERN, Organisation européenne pour la recherche nucléaire, CH-1211 Genève, Switzerland*
[b] *IES, Institut d'Electronique et des Systèmes, 34095 Montpellier, France*
[c] *LIRMM, Laboratoire d'Informatique, de Robotique et de Microélectronique de Montpellier, 34095 Montpellier, France*
[d] *CNRS, Centre National de la Recherche Scientifique, 75794 Paris, France*

E-mail: Rudy.Ferraro@cern.ch

Abstract: The need for upgrading the Total Ionizing Dose (TID) measurement resolution of the current version of the Radiation Monitoring system for the LHC complex has driven the research of new TID sensors. The sensors being developed nowadays can be defined as Systems On Chip (SOC) with both analog and digital circuitries embedded in the same silicon. A radiation tolerant TID Monitoring System (TIDMon) has been designed to allow the placement of the entire dosimeter readout electronics in very harsh environments such as calibration rooms and even in the mixed radiation field such as the one of the LHC complex. The objective of the TIDMon is to measure the effect of the TID on the new prototype of Floating Gate Dosimeter (FGDOS) without using long cables and with a reliable measurement system. This work introduces the architecture of the TIDMon, the radiation tolerance techniques applied on the controlling electronics as well as the design choices adopted for the system. Finally, results of several tests of TIDMon under different radiation environments such as gamma rays or mixed radiation field at CHARM are presented.

Keywords: Radiation damage monitoring systems; Radiation damage evaluation methods; Radiation damage to electronic components; Dosimetry concepts and apparatus

[1] Corresponding author.

doi:10.1088/1748-0221/12/04/C04007

Contents

2017 JINST 12 C04007

1 Introduction

The complex radiation environment of the Large Hadron Collider (LHC) tunnels and its surrounding areas is composed of several types of particles over a broad range of energies, from a few meVs (i.e. thermal neutrons) up to GeVs [1]. The electronic equipment operating in such a harsh radiation environment, mostly based on Commercial Off The Shelf (COTS) components [2], can be affected by radiation effects. The monitoring of the accumulated radiation levels is a crucial task in order to anticipate and study the equipment failures and long-term degradation. At CERN, monitoring of the Total Ionizing Dose (TID) is performed by the Radiation Monitor (RadMON) system by means of RadFET (Radiation Sensing Field Effect Transistors) dosimeters [3]. The RadMon, which utilises a 100 nm RadFET dosimeter, can achieve a dose resolution of 6 rad (Si). To increase the resolution of the TID monitoring of the RadMON system, a new candidate as TID-detector, which is based on floating gate MOS transistor, is currently investigated. To study the suitability of the sensor for CERN application, it is necessary to have a system that allows to fully characterise all the parameters of the sensor under a representative mixed radiation field.

For this purpose, a radiation tolerant TID Monitoring (TIDMon) system has been designed to measure the effect of the TID on the Floating Gate Dosimeter (FGDOS). The architecture of the system has been developed to be a multi-purpose precision instrument capable of measuring and diagnostic several analogue and digital signals in radiation environments, such as the FGDOS. The TIDMon system is composed of COTS components, which have been individually tested under radiation with protons, gamma rays, and 1 MeV neutrons. The architecture is based on an FPGA and allows the remote control of the sensor parameters. To calibrate the FGDOS sensors, it is necessary to have a reference dose measurement, for this purpose, a part of the TIDMon system

is dedicated to measure the TID, by means of the same sensor as the RadMon: the RadFET. The radiation response of the RadFET in mixed radiation environment has been extensively studied in [4]. Therefore it will be used as a reference to compare directly with the TID measured by the FGDOS sensor.

The FGDOS sensor have been conceived as a prototype and produced by ICMalaga. The FGDOS is a system on chip (SoC) fabricated in a standard CMOS technology that embeds a floating gate transistor and its readout circuitry. The circuitry is composed of a current to frequency converter that provides a square wave signal output whose frequency is proportional to the drain current of an N-MOS transistor that reads the floating gate voltage. Prior to irradiation, the floating gate is charged through an injector of charge carriers exploiting the tunnelling effect. During the irradiation, the charges stored in the floating gate are neutralised by the radiation-induced charges created in the silicon oxide. This effect induces a floating gate potential variation and thus, a frequency variation on the output of the FGDOS. Once the floating gate is discharged due to the TID effect, it can be charged back to its initial value by injecting again positive charges on the floating gate. In this way, the TID is monitored by measuring the frequency of the square wave signal. The working principle of the FGDOS is widely described in [5]. Furthermore, the FGDOS contains internal configuration registers accessible by an SPI communication interface that allow modifying the configuration parameters. One of these parameters allows to bypass the "current to frequency" converter and directly measure the drain current of the N-MOS transistor induced by the floating gate potential. In addition to the floating gate, the sensor also embeds a standard MOSFET having the same size and oxide thickness as the floating gate. Consequently, the MOSFET FG is sensitive both to the effects of temperature and radiation, while the standard MOSFET, hereafter named reference MOSFET, is sensitive to temperature but negligently to radiation effects. In the same way as for the floating gate, the chip provides a second signal output whose the frequency is proportional to the reference MOSFET. As describe in [6] this output can be used to compensate the temperature effect on the floating gate.

The FGDOS radiation response curve is nonlinear because of its working principle. To overcome this constraint, a recharge process has been developed to force the sensor to operate in small part of its response curve to increase the radiation response linearity. The linearity achieved by this recharge process has been characterized with gamma-ray irradiation campaigns. The entire system has been tested with gamma-ray irradiation and under mixed radiation fields at CHARM (Cern High energy AcceleRator Mixed field facility at CERN) [7] and its reliability is investigated.

2 Design choices for the TIDMon

The architecture of the TIDMon, depicted in figure 1. is built around a Flash-based FPGA (Actel ProAsic3), which has been chosen for the inherent robustness of its configuration memory to Single Event Upsets (SEUs) [8]. The choice to prefer a Flash-based FPGA rather than an SRAM-based FPGA which can withstand a higher ionising dose, has been motivated by the fluxes of the mixed-field radiation environment of CHARM. Since this facility is designed to perform accelerated radiation tests by producing high particle fluxes, the large number of SEUs generated in an FPGA with a sensitive configuration memory such as the SRAM-based FPGA would be very challenging to manage.

2017 JINST 12 C04007

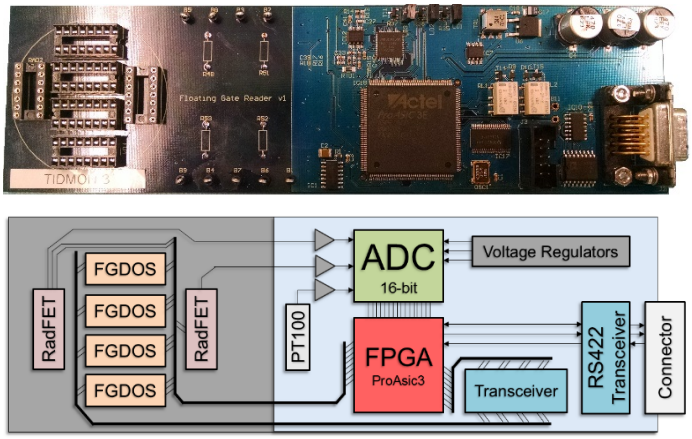

Figure 1. TIDMon board and general hardware architecture with on the right the Tester part and on the left the DUTs part.

The test board has six sockets for the TID sensors; four dedicated to FGDOS sensors and two dedicated to RadFET dosimeters. An analogue acquisition chain, which is composed of an 8-channels 16-bit ADC, two adjustable current sources and operational amplifier circuits, allows biasing the RadFETs in weak inversion mode and measure the voltage threshold shift due to TID [9]. The current sources are configured for the operating conditions of the RadFET, but they can be adjusted to characterize any kind of analogue components that are current driven (e.g. diodes, bjt, etc). To monitor the level of operational degradation of the board, a diagnostic circuit has been embedded, too. The voltage regulators output and the board temperature are also measured by the ADC. The system uses a serial link to transfer the data to the test computer in real time.

For the FGDOS, the readout and recharge procedures are digital and are performed by a controller implemented in the FPGA, described in the next section. The full range of the radiation response of the sensor goes from 0 Hz when the floating gate is completely discharged up to 250 kHz when it is completely charged and is non-linear. The purpose of the FGDOS controller is to linearize the sensor response by forcing it to work on a small part of its full-scale response. The controller achieves this by continuously recharging the FGDOS to a specific charge level when it is discharged below a specific threshold, as shown in figure 2. According to [10], the nominal frequency operating range is around 32–49 kHz and the sensitivity obtained in this range is around 320 Hz/rad(Si). During the charge phase, it is not possible to measure the effect of TID. Consequently, on the TIDMon the injection voltage has been set to the maximum (19 V), which correspond to a recharge rate about 20 kHz/s, in order to minimise the charge time.

The RadFETs readout procedure is the same as the RadMON system [11] and requires different configurations during the readout and the irradiation phases. They are applied by the FPGA by means of switches, as depicted in figure 3. During the readout procedure, the RadFET is put in weak inversion mode. Since it is a P-MOS transistor, the gate and the drain are both shorted to ground and the RadFET is supplied by a constant current source adjusted to 10 μA for 100 ms, according to the response time of the sensor. In this configuration, with a small current the VGS voltage is practically equal to the threshold voltage. Once the threshold voltage measurement is done, the source and the gate are grounded. During this time, the gate can be biased at 5 V to

2017 JINST 12 C04007

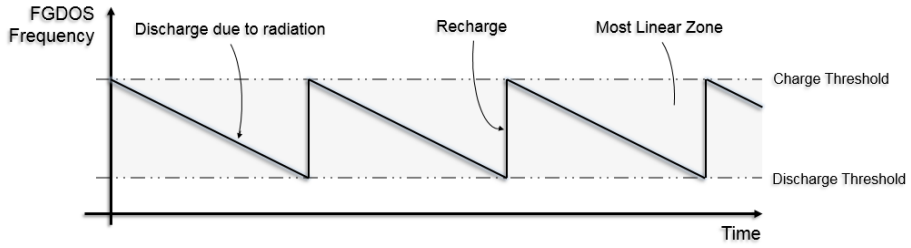

Figure 2. Functional operation of the automatic recharge procedure of the FGDOS during irradiation.

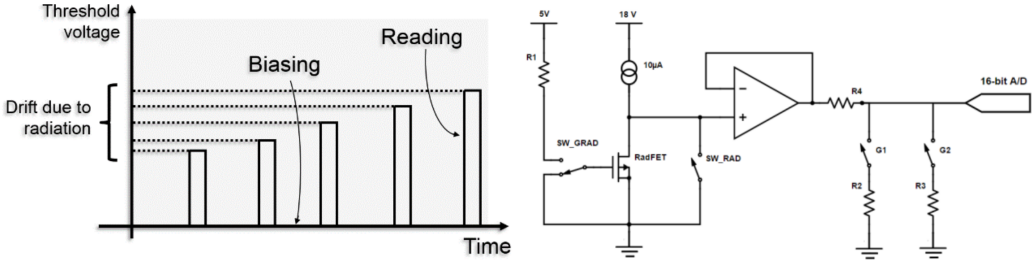

Figure 3. Readout procedure and circuitry for the RadFET.

increase the radiation sensibility of the RadFETs as is described in [10]. The adjustable attenuation of the analogue acquisition chain made by the resistance network allows exploiting the full range of the sensors.

3 FPGA architecture

The architecture of the FPGA has been designed to be as generic as possible in order to have an internal design that can be re-used to drive other TID sensor candidate. One part of the design can be referred as a "generic tester", which is dedicated to the board management, and another part is dedicated more specifically to drive the Devices Under Tests (DUTs), which are in this case the RadFET and FGDOS sensors, as shown in figure 4. The architecture of the "generic tester" part is built around a low gate count controller for Advanced Microcontroller Bus Architecture (AMBA)

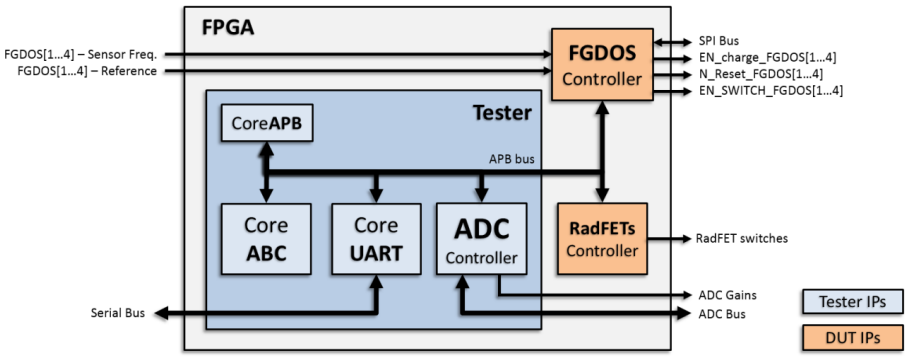

Figure 4. TIDMon FPGA architecture with in blue the generic IPs provide by the tester structure and in orange the IPs dedicated to the DUTs.

called CoreABC [12]. The CoreABC controls the slave peripherals through an APB bus. The controller can be programmed with simple user routines that are written in assembler language and are directly converted into logic elements in the FPGA and not stored in a RAM. The readout routine reads the sensors and ADC data and transfers them every second through the UART serial controller. The cores provided by the FPGA vendor, in addition to facilitating the tester development, have the advantage to have a configurable architecture, which allows adjusting their features to the needs of the application, and thus the amount of resources used by the core and its complexity that can lead to a reduction of its radiation sensitivity. Particularly for the CoreABC where many parts of the design can be reduced or removed, as the size of the instruction address register, the part of the design dedicated to manage interruptions or the use of an accumulator register. Another advantage is the accessibility of the core codes, which allows applying mitigation techniques to reduce further their radiation sensitivity. The DUTs part of the architecture is composed of independent APB based controllers dedicated to each DUT. The DUT's controllers have internal registers that allow the CoreABC to read the sensor's data and modify the DUT's configuration. This architecture allows to easily develop new DUT's controllers that can be interfaced to the APB bus, in order to study different kinds of sensors trough this system. The system can also be used to test the robustness of the DUT's controller to radiation before their implementations on a final system using the same family of FPGA as is the case for the target system of the FGDOS sensor: the RadMon.

Two DUT controllers have been implemented for this project: the RadFET controller, which simply applies the readout protocol shown in figure 3, and the FGDOS controller, which is detailed in the next section.

3.1 FGDOS controller

The FGDOS controller is based on six processes; the Edge Detector, the Pulse Counter, the charge process, the SPI Controller and the IOs controller, as shown in figure 5.

The Frequencies meter process calculates the sensors' frequencies by counting the pulses sent by the Edge detector on rising edge detection. The process is composed of two parts that calculate the frequency at different speeds and precisions to cover different objectives. The objective of the first part is to provide an accurate calculation of the sensor frequency. The TIDMon system will then transmit this frequency to a remote computer that will accurately calculate the corresponding dose. This part counts the number of pulses sent by the edge detector during one second, and thus provides a frequency with a resolution of 1 Hz, which should theoretically give a dose resolution of 3.2 mrad (Si). As explained previously, the level of the voltage injection has been configured to charge the floating gate with the maximal recharge rate (around 20 kHz) in order to reduce to the minimum the blind time. To avoid overcharging the sensor, which would imply loss of linearity, it

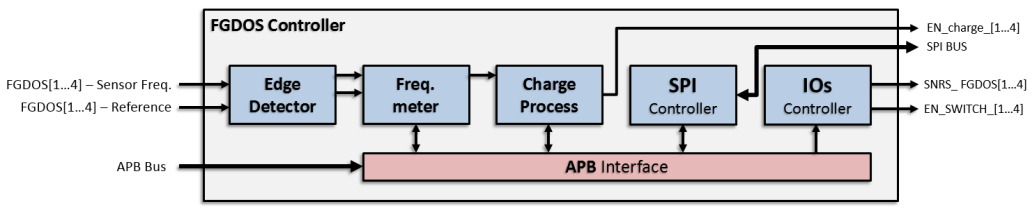

Figure 5. FGDOS controller architecture.

is necessary to have a very fast calculation of its frequency. For this purpose, the second part of the frequency meter process counts the number of pulses during 15 ms and therefore provides in 15 ms a frequency with an accuracy of 128 Hz.

The recharge process of the sensor can be carried out in two modes; a manual mode and an automatic mode. The manual recharge mode allows the user to charge the sensor manually to a specific point or to the maximum. In this mode, the sensor will not be recharge after its complete discharge. In automatic mode, the FGDOS is automatically charged to a target when the sensor frequencies goes below a discharge threshold as shown in figure 2. These two values, stored in the controller registers, allow the user to define the operating range of the sensor to increase the linearity of the radiation response of the sensor. The target and the threshold have been set by default to 32 and 49 kHz. The SPI controller contains the SPI commands that allow reading and writing the internal registers of the sensor. Through a configuration register, the internal current to frequency converter of the sensor can be bypassed and thus the output provides directly the drain current of the N-MOS transistor reader of the floating gate. In this case, the IOs Controller allows redirecting the outputs of the sensors using switches to test pins to measure the current variations with external instruments. The APB Interface contains the internal registers of the FGDOS controller and manages the communication with the APB bus.

4 Radiation assurance

The TIDMon has been designed to work up to a TID of at least 22 krad (Si). The digital components, such as the FPGA, the RS422 Transceiver, the ADC and the DUT transceiver have been carefully selected and tested individually under radiation against the TID, Single Event Effects (SEEs) and displacement damage (DD) effects with 230 MeV protons (up to $9 \cdot 10^{11}$p/cm^2) and 1 MeV neutrons (up to $4 \cdot 10^{12}$n/cm^2) [13].

The weakest part of the system is the ADC which stops working at about 22 krad (Si) as shown in table 1. Beyond this dose the ADC is not able to provide voltage measurements. The consequence of this failure is the loss of the entire analogue chain, and thus the loss of the dose monitoring through RadFETs. After this failure, the TIDMon can continue to operate in "degraded mode", by measuring the dose only with the FGDOS, which necessitates only the FPGA and the 19 V regulator to work. In this mode, without the reference dose provided by the RadFET, the system can no longer be used to investigate or calibrate the effect of the dose on the FGDOS but it can still be used as a dosimetry system with calibrated FGDOS dosimeters. After 22 krad (Si) the next system failure is also due to the ADC which present a huge increase of its current consumption. The current consumption can reach about 800 mA at 35 krad (Si) instead of the 50 mA in nominal conditions as demonstrate in [10], and thus damage the 5 V voltage regulator and lead to the complete failure of the system. The second life-limiting component is the FPGA, which can withstand in the best case a dose of 40 krad (Si) before the complete failure as shown in table 1.

Concerning the degradation of the performance of the system, the electronic hardware of the analogue part is based on the same hardware as the RadMon V6, which have been tested besides of 230 MeV protons and 1 MeV neutrons, with a ^{60}Co source as described in [10]. The critical parameters for the accuracy of the RadFETs voltage threshold measurement are the 18 V regulator that supply the current sources, the current sources, the OpAmp which attenuates the voltage for the ADC and the voltage reference of the ADC. As shown in table 2, the 18 V regulator exhibited a

2017 JINST 12 C04007

Table 1. Cross section and lifetime of the digital components obtain with a proton beam irradiation with a fluence of $9 \cdot 10^{11}$ p/cm^2 and a corresponding total ionising dose of 50 krad.

Part	Cross section	Lifetime [rad(Si)]
RS422 Transceiver	no SELs observed no SEUs observed	Rather as at least of 50k
DUT Transceiver	no SELs observed no SEUs observed $7.6 \cdot 10^{-11}$ cm^2/device (SEUs)	Rather as at least of 40k
16-bit ADC	$9.5 \cdot 10^{-12}$ cm^2/channel (SEUs) no SEL observed $5.6 \cdot 10^{-14}$ cm^2/bit (FFs SEUs)	22k
FPGA ProASIC3	$4.6 \cdot 10^{-14}$ cm^2/bit (RAMs SEUs) no SEL observed	35k–40k

drift lower than 0.4 % respect to the nominal value up to 50 krad (Si). The current source exhibited a drift lower than 4.9 % up to 50 krad (Si) with cobalt and lower than 7.5 % up to 30 krad (Si). Tests has been performed with RadFET and the current source under 220 MeV protons up to 30 krad (Si) and no clear evidence of a direct impact of this drift on the RadFETs radiation response has been observed. For the measure of the RadFET voltage, the OpAmp shown a maximal drift of 0.2 % up to 50 krad (Si) with cobalt and the voltage reference of the ADC do not exhibit a significant variation until its complete failure at about 22 krad (Si). If we consider that the ADC allows to read the dose only up to 22 krad (Si), up to this point the impact of the degradation of the analog circuitry on the RadFET dose measurement is negligible. For the FGDOS dose measurement, the only analogue component that can suffer from degradation due to the dose is the 19V regulator. This regulator is the same as the 5 V and the 18 V with a different configuration, it has not been tested in the 19 V configuration but we assume that the behaviour should be very close to the 18 V degradation. In any case, the degradation of the 19 V regulator will not affect the response of the FGDOS measurement, but only the recharge rate of the FGDOS. A significant deterioration of the regulator would only lead to an increase of the recharge time of the sensor, but it will remain operational. Moreover, the temperature of the board, the degradation the current sources and the voltages regulator voltages are continuously monitored by the ADC to verify that the parameters stay in the specifications.

The sensitivity of the FPGA against the SEUs is around $5 \cdot 10^{-14}$ for the flip-flops and the SRAM level as shown in table 1. To make the FPGA design radiation tolerant a Triple Modular Redundancy (TMR) mitigation technique is applied automatically on all the design at registers level by means of a commercial synthesis tool. In return, the number of resource used has doubled. The RAM blocks of the CoreABC have been triplicated manually in the code because the tool is not able to do it.

No destructive failures due to latch-up have been observed on all the components up to $9 \cdot 10^{11}$p/cm^2 with 220 MeV protons.

5 Experimental results

In this section, the performances of the recharge process achieved by the TIDMon system in the CC60 facility and the ability of the system to monitor the TID in the CHARM mixed-field facility

2017 JINST 12 C04007

Table 2. Variation of the parameters of the analogue components to a TID of 50 krad (Si) — ^{60}Co source, 1 MeV equivalent neutron fluence of $4 \cdot 10^{12}$n/cm^2 and with a 220 MeV proton beam at different doses.

Part	^{60}Co	1Mev neutron	220Mev Protons
OP Amp	V_{out} = 0.2%	V_{out} = 0.2%	V_{out} = 0.1% @ 20krad(Si)
Positive Voltage reg. 5 V	V_{out} = 0.5%	V_{out} = 2.0%	V_{out} = 4.5% @ 32 krad(Si)
Positive Voltage reg. 18 V	V_{out} = 0.4%	V_{out} = 2.0%	Not tested in this configuration
Curent source 10 μA	I_{out} = 4.9%	I_{out} = 15%	I_{out} = 7.5% @ 30 krad(Si)

are presented. The qualification of the different aspects of the FGDOS (radiation and temperature sensitivity, sensor and batch response variation) and its suitability in these different environments are discussed in details in [14].

5.1 Gamma rays irradiation

The CERN CC60 facility generates a gamma-ray radiation field by means of a 60 Cobalt source. FGDOS sensors have been irradiated at a dose rate of 320 rads (Si)/h in the order to investigate the linearity of the radiation response obtained with the auto-recharge process and the behaviour of the TIDMon system. The irradiation tests were performed with two TIDMon boards, which have cumulated respectively 8 and 5 krad(Si). During the tests, none of the two boards showed significant variation nor of the critical parameters of the analogue parts neither their power consumption, which is in agreement with the tests performed at component-level.

Without the automatic recharge process, if the sensor previously charged to the maximum is irradiated to its full range, the radiation response obtained is non-linear, as is it shown by the red curve in figure 6. With the automatic recharge process, the sensor is forced to work in a small part of the full-scale response in order to reduce its non-linearity. The nominal operating range has been identified between 32 kHz and 49 kHz. In this way, the sensor is charged before the irradiation to 49 kHz and when the frequency exceeds the lower limit because of the dose, the sensor is charge back to 49 kHz. Thus the same part of the full-scale response is repeatedly used. The see-saw signal obtained with this process is shown by the blue curve in figure 6. The jumps are then compensated to obtain the read curve in figure 6, where only the frequency variation is due to the dose. To compare the linearity of the original full-scale curve with the compensated curve obtained by the auto-recharge process, the compensated curve has been adjusted to the same starting point.

The percentage of non-linearity of the two radiation response curves has been evaluated by calculating the maximum difference, between the sensor curves and their corresponding linear fitting curves. The linear fitting curve is defined as a line having a slope equal to the average sensitivity of the radiation response. According to this definition, over a cumulated dose of 2.0 krad(Si), the percentage of non-linearity achieved by the automatic recharge process is lower than 1.8% where the percentage of non-linearity of the full range response is about 26%. The left graph of the figure 6 show with several sensors the ability of the recharge process to reach the charge target with a precision of 128 Hz, which has no significant impact on the linearity achieved by the process.

The radiation sensitivity obtained with the auto recharged response curve is around 340 Hz / rad(Si). Considering the intrinsic FGDOS sensor noise of 5 Hz, the TID measurement resolution obtained by the TIDMon system using the FGDOS sensor is 15 mrad(Si). The recharge rate of the FGDOS with an injection voltage of 19 V is around 20kHz/s and allows recharging the sensor in

2017 JINST 12 C04007

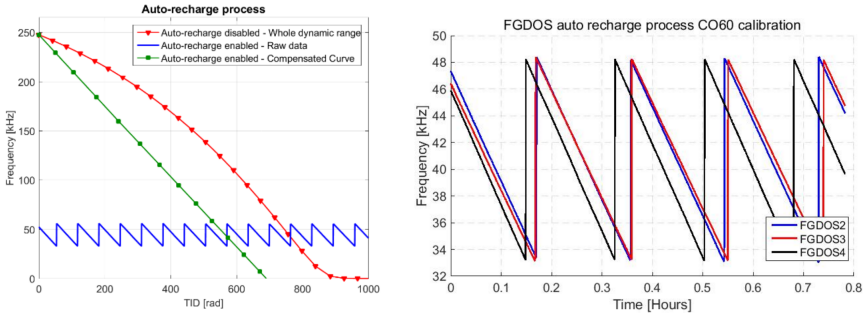

Figure 6. Effect of the Auto-recharge process on the radiation response. On the left figure, the blue curve represents the radiation response with auto-recharge process, the green curves the same response recharge compensated and the red the whole dynamic range of the FGDOS. On the right the accuracy of the recharge process is shown with three different sensors.

less than 2 seconds, reducing the blind time at 2 seconds every 59 rads (Si). The blind time can be completely avoided by using FGDOS sensors with asynchronous recharge rate.

5.2 Mixed field irradiation

In order to investigate the suitability of the FGDOS in mixed-field environments and the reliability of the TIDMon to operate in harsh environments, irradiations have been performed at CHARM with different mixed-fields. Here, the radiation field is induced by the interaction of a 24 GeV proton beam extracted from the Proton Synchrotron (PS) with a copper or aluminium target. According to the test position chosen and the type of target, it is possible to achieve different fields in terms of spectrum and intensity. Moreover, the field spectrum can be modulated by selecting the configuration of movable shielding that can be placed between the target and the test positions [7]. 100nm RadFETs biased to 5 V have been used during these tests to evaluate the reliability of the TID measured by the FGDOS. As described in [4], the dose can be measured in mixed particle field by means of 100nm RadFETs calibrated with gamma rays with an uncertainty of ±25%. According to this value, the TID measured with FGDOS in the mixed particle field of CHARM in different configurations are in agreement with the TID measured by the RadFET, as shown in figure 7.

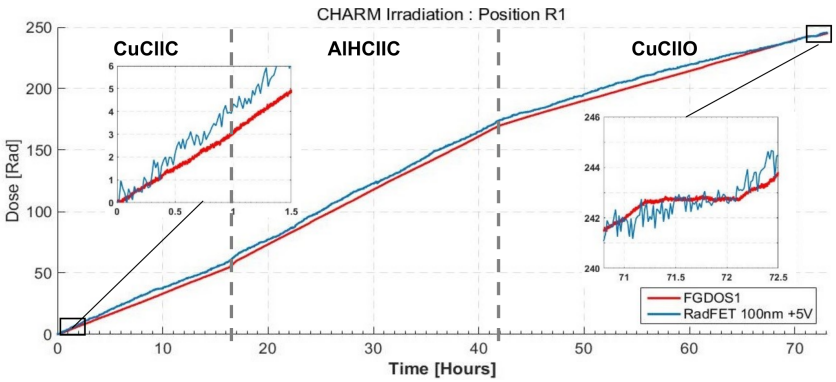

Figure 7. TID measured in position 1 by FGDOS and RadFET (biased to +5 V) dosimeters with three different configurations of CHARM. The copper target is labelled Cu and the aluminium with holes target is labelled AlH. The last four characters are the configuration of the shielding ("C" = Concrete block, I = Iron block and O = No block).

2017 JINST 12 C04007

The TIDMon using FGDOS allows achieving a dose measurement with a higher resolution than the dose measured by the RadFETs, as shown in the first highlighted zoomed area box. In the second one, the beam stop is clearly visible through the FGDOS measurement, where the dynamic of the RadFET masks it.

6 Conclusions

The TIDMon system, conceived to measure the effect of the total ionizing dose on analogue and digital components capable of being used as dosimeters, as the new prototype of floating gate dosimeter has been presented. The presented modular architecture of the system allows to easily generate new DUT controllers. In particular, the controller of the FGDOS-based detector has been introduced. The suitability of the overall monitoring system to operate in harsh radiation environments up to 22 krad (Si), and up to 30 krad (Si) in degraded mode, has been verified with irradiation campaigns at component-level and at system-level with two irradiation campaigns at CC60 and CHARM facilities. The sensitivity, the availability and the linearity of the FGDOS sensor achieved through a recharge process implemented by the controller have been characterized in the CC60 facility of CERN.

The relevance of the TID measurement of the FGDOS in mixed-fields has been demonstrate through experiments performed at CHARM with different configurations of the facility and compared with RadFETs measurements in same conditions.

We intend to use further the TIDMon system to characterize other promising TID sensor candidates. For example, a low cost commercial NMOS transistor that shown a sensitivity similar to the RadFET is currently under characterization to determine if it can be used as a TID sensor.

References

[1] K. Roeed, M. Brugger and G. Spiezia, *An overview of the radiation environment at the LHC in light of R2E irradiation test activities*, CERN-ATS-Note-2011-077 (2011).

[2] F. Faccio, *COTS for the LHC radiation environment: the rules of the game*, talk given at the 6th *Workshop on Electronics for LHC Experiments*, September 11–15, Krakow, Poland (2000).

[3] G. Spiezia et al., *The LHC radiation monitoring system — RadMon*, PoS(RD11)024.

[4] J. Mekki et al., *Mixed particle field influence on RadFET responses using Co-60 calibration*, *IEEE Trans. Nucl. Sci.* **60** (2013) 2435.

[5] E. Garcia-Moreno et al., *Floating gate CMOS dosimeter with frequency output*, *IEEE Trans. Nucl Sci.* **59** (2012) 373.

[6] E. Garcia-Moreno et al., *Temperature compensated floating gate MOS radiation sensor with current output*, in IEEE Transactions on Nuclear Science, vol. 60, no. 5, pp. 4026-4030, Oct. 2013.

[7] J. Mekki et al., *CHARM: a mixed field facility at CERN for radiation tests in ground, atmospheric, space and accelerator representative environments*, *IEEE Trans. Nucl. Sci.* **63** (2016) 2106.

[8] M. Wirthlin, *High-reliability FPGA-based systems: space, high-energy physics, and beyond*, *IEEE Proc.* **103** (2015) 379.

2017 JINST 12 C04007

[9] S. Metzger et al., *Study of parameters influencing the response of RADFETs*, in the proceedings of the 14th *European Conference on Radiation and Its Effects on Components and Systems (RADECS)*, September 23–27, Oxford, U.K. (2013).

[10] S. Danzeca et al., *Characterization and modeling of a floating gate dosimeter with gamma and protons at various energies*, *IEEE Trans. Nucl. Sci.* **61** (2014) 3451.

[11] G. Spiezia et al., *A new RadMon version for the LHC and its injection lines*, *IEEE Trans. Nucl. Sci.* **61** (2014) 3424.

[12] Microsemi, *CoreABC v3.5 Handbook*, available at http://www.actel.com/ipdocs/CoreABC_HB.pdf.

[13] G. Spiezia et al., *Compendium of radiation-induced effects for candidate particle accelerator electronics*, in the proceedings of the *IEEE Nuclear and Space Radiation Effects Conference*, July 17–21, San Francisco, U.S.A. (2013).

[14] M. Brucoli et al., *Floating gate dosimeter suitability for accelerator-like environments*, submitted to *IEEE Trans. Nucl. Sci.* (2016).

2017 JINST 12 C04007